OMTON, Volume *32*

Supplemental information

Intra-tumoral administration of CHST15 siRNA remodels tumor microenvironment and augments tumor-infiltrating T cells in pancreatic cancer

Juanjuan Ye, Futoshi Suizu, Keiko Yamakawa, Yuri Mukai, Hiroyuki Yoneyama, Jiro Kondo, Motohiko Kato, Akira Nishiyama, Naohisa Yahagi, and Kyuichi Kadota

Supplemental Materials and Methods

In vitro silencing experiments

BxPC-3 cells (human PDAC cell line) were purchased form ECACC. The concentration of CHST15 siRNA was 50 nM. Five hundred μL/well of Opti-MEMl (GIBCO), siRNA and 7.5 μL/well of RNAiMAX-Reagent (Invitrogen) were incubated on a 6-well plate at 25°C for 20 minutes. BxPC-3 cells were suspended in 2.5 mL of the basic culture medium in a CO_2 incubator for 48 hours (2.5 mL/well). Total RNA was extracted from each transfected cell using a FastPure RNA kit (Takara Bio Inc.) according to the manufacturer's instructions. The cDNA was synthesized and real-time RT-PCR was performed using SYBR premix Taq (Takara Bio Inc.). The expression of the human CHST15 gene was normalized by the expressed amount of RNA of human GAPDH[1-3].

In vitro cell proliferation and invasion assay

Cell proliferation was measured by WST-1 assay as described previously[3]. Cell invasion was assessed using the CytoSelect 24-well Cell Invasion Assay (CELL BIOLABS, Inc., San Diego, CA). The lower chambers were filled with DMEM containing 10% FBS, and cells (2×10^4 cells/300 μL) in serum-free DMEM were placed in the upper chamber. After incubation for 24 h, invasive cells on the bottom of the invasion membrane were stained and quantified at OD 560nm in accordance with manufacture's instruction.

In vivo RISC-loading of and CHST15 mRNA cleavage by intratumorally injected CHST15 siRNA in BxPC-3 xenograft model

To determine the dosing interval of *in vivo* CHST15 siRNA, stem-loop PCR followed by RNA immunoprecipitation and *in situ* hybridization (ISH) were performed. Human PDAC cell line BxPC-3 cells (ECACC 93120816) were used. BxPC-3 cells ($1x10^7$ cell/mouse) were implanted subcutaneously to T cell-deficient Balb/c-nu mice on day 0. Single injection of CHST15 siRNA (10 nmol/L, n=6) or physiological saline as control vehicle (n=6) was performed intratumorally (100 μL/mouse) at day 12 and mice were sacrificed at days 14 (n=3/each) and 17 (n=3/each). This study was approved by the Institutional Animal Care and Use Committee (Approval No. IACUC649-009) and was performed in accordance with the animal welfare bylaws of Shin Nippon Biomedical Laboratories, Ltd., which is accredited by AAALAC International.

For stem-loop PCR followed by RNA immunoprecipitation, frozen tissues from day 17 [day 5 after dosing] were used. Ago2-binding RNA was purified from tumor tissue samples using MagCapture™ microRNA isolation kit, human Ago2 (FIJIFILM Wako Pure Chemical Corporation) according to the manufacture's instruction. Ago2-loaded siRNA was then quantified by stem-loop qPCR based on previously published methods[4, 5]. The following primers were used: antisense RT primer: GTCGTATCCAGTGCAGGGTCCGAGGTATTCGCACTGGATACGACATGGAG, sense RT primer: GTCGTATCCAGTGCAGGGTCCGAGGTATTCGCACTGGATACGACCTGATT, antisense forward primer: CGCGATTGTATTCATCTTGCTCTG, sense forward primer: CGCGGAGCAGAGCAAGATGAATAC, universal reverse primer: GTGCAGGGTCCGAGGTATTCG.

For ISH, formalin fixed paraffin embedded tissues samples from day 14 [day 2 after dosing] were used. BaseScope™ LS Red ISH assay (Advanced Cell Diagnostics, CA. USA) was performed by the manufacturer[6, 7]. For the detection of the CHST15 mRNA cleavage site by hCHST15 siRNA, short length probe was designed as follows: CAGCTCTGCAAAGGAGCAGAGCAAGATGAATACAATCATTATCGG. The cleavage site-containing mRNA was visualized as a dot led and the number of tumor cells positive for red signals in 5 filed/section at 400-fold magnification were measured using ImageJ software (National Institute of Health).

Table S1. List of primary antibodies used in the present study

Antibody [clone]	Source	Dilution
Rabbit anti-human CHST15 pAb	Merk	50
Rabbit anti-Citrullinated Histone H3 pAb	Abcam	5,000
Rabbit anti-mouse CD31 pAb	Abcam	100
Rat anti-mouse Ly6C/G mAb [RB6-8C5]	Arigo	50
Rabbit anti-mouse CD3 mAb [SP7]	Abcam	1,000
Rabbit anti-mouse CD8α mAb [EPR20305]	Abcam	1,000
Rabbit anti-mouse CD4 mAb [EPR19514]	Abcam	2,000

Table S2. Melting temperature of the hybridized complexes between an antisense oligonucleotide (ASO) and its target RNA sequences

Complex	Sequence *	MM	T_m (ºC)
Human/ASO	5'-GGAGCAGAGCAAGATGAAT-3' 3'-CCUCGUCUCGUUCUACUUA-5'	0	73
Pig/ASO	5'-GGA<u>A</u>CAGAGCAAGATGAAT-3' 3'-CCU<u>C</u>GUCUCGUUCUACUUA-5'	1	65
Rat/ASO	5'-G<u>C</u>AG<u>AC</u>GAGCAAGATGAAT-3' 3'-C<u>C</u>UC<u>GU</u>CUCGUUCUACUUA-5'	3	57
Mouse/ASO	5'-G<u>C</u>AGC<u>CC</u>AGCAAGATGAAT-3' 3'-C<u>C</u>UCG<u>UC</u>UCGUUCUACUUA-5'	3	54

* Mismatch (MM) bases are underlined.

A

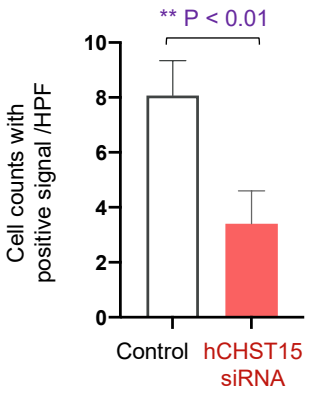

Day 2 post single dosing of vehicle control or hCHST15 siRNA.

B

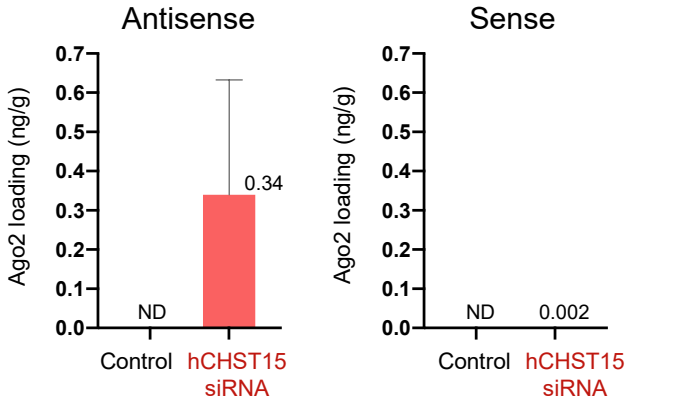

Average values (ng/g) are shown in the hCHST15 siRNA-treated mice (n=3) at Day 5 post single dosing.
N.D.: Not detected in the vehicle control-treated mice (n=3)

Figure S1. Cleavage of hCHST15 siRNA-binding site of CHST15 mRNA (A) and detection of RISC-loading sense and antisense strands of hCHST15 siRNA in tumor cells in vivo in human PDAC BxPC-3 cells.
A: Quantitative analysis of stained tissues by ISH. Short human mRNA sequence containing hCHST15 siRNA-cleavage site was stained by BaseCoreTM Red ISH assay. The number of cells with positive signals are shown. Mean ± SD (n=3). **p <0.01 by independent t test. **B:** RICS-loading sense or antisense strand of hCHST15 siRNA was measured by stem-loop PCR. Average values (ng/g) are shown in the control- or hCHST15 siRNA-treated mice (n=3). N.D.: Not detected in the Saline-treated mice (n=3).

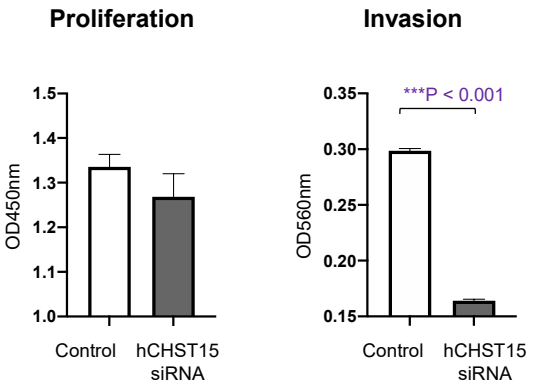

Figure S2. hCHST15 siRNA did not affect proliferation of BcPC-3 cells in vitro.
(Left) Proliferation of BxPC-3 cells treated with Saline as a control or 50 nM of hCHST15 siRNA. Mean ± SD (n=5). Not significant by Wilcoxon rank sum test. (right) Invasion of BxPC-3 cells treated with Saline as a control or 50 nM of CHST15 siRNA. Mean ± SD (n=2). ***p < 0.001 by Wilcoxon rank sum test.

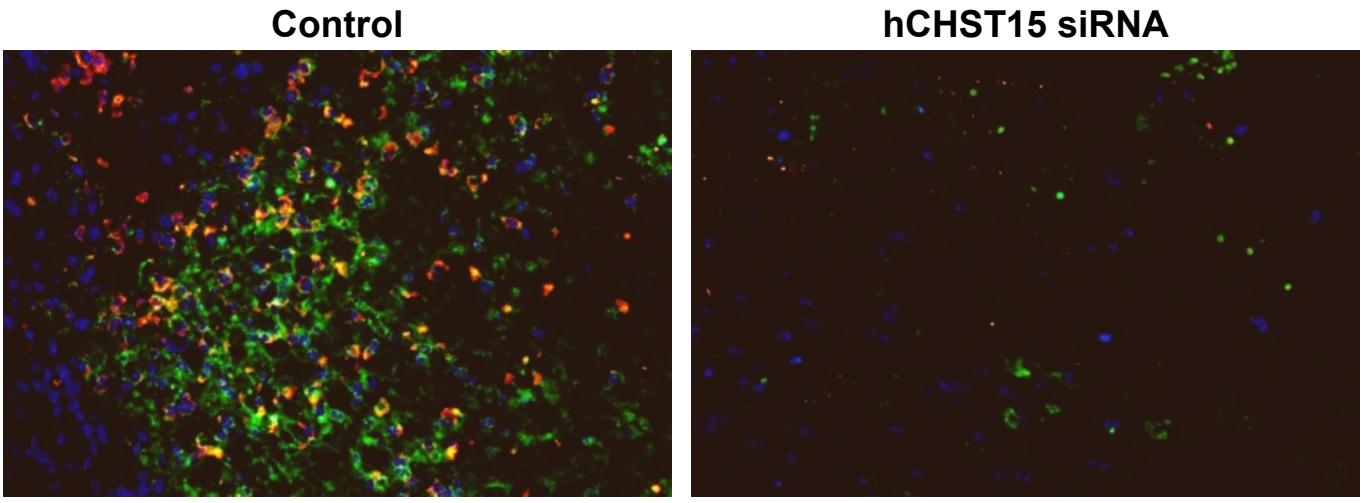

Figure S3. Part of tumoral MDSC expressed CHST15 and hCHST15 siRNA repressed MDSCs in the tumor. Immunostaining for CHST15 (red) and Ly6C/G (green) with DAPI (blue) in the tumor of KPC mice treated with control (left panel) or hCHST15 siRNA (right panel). Original magnification, x400.

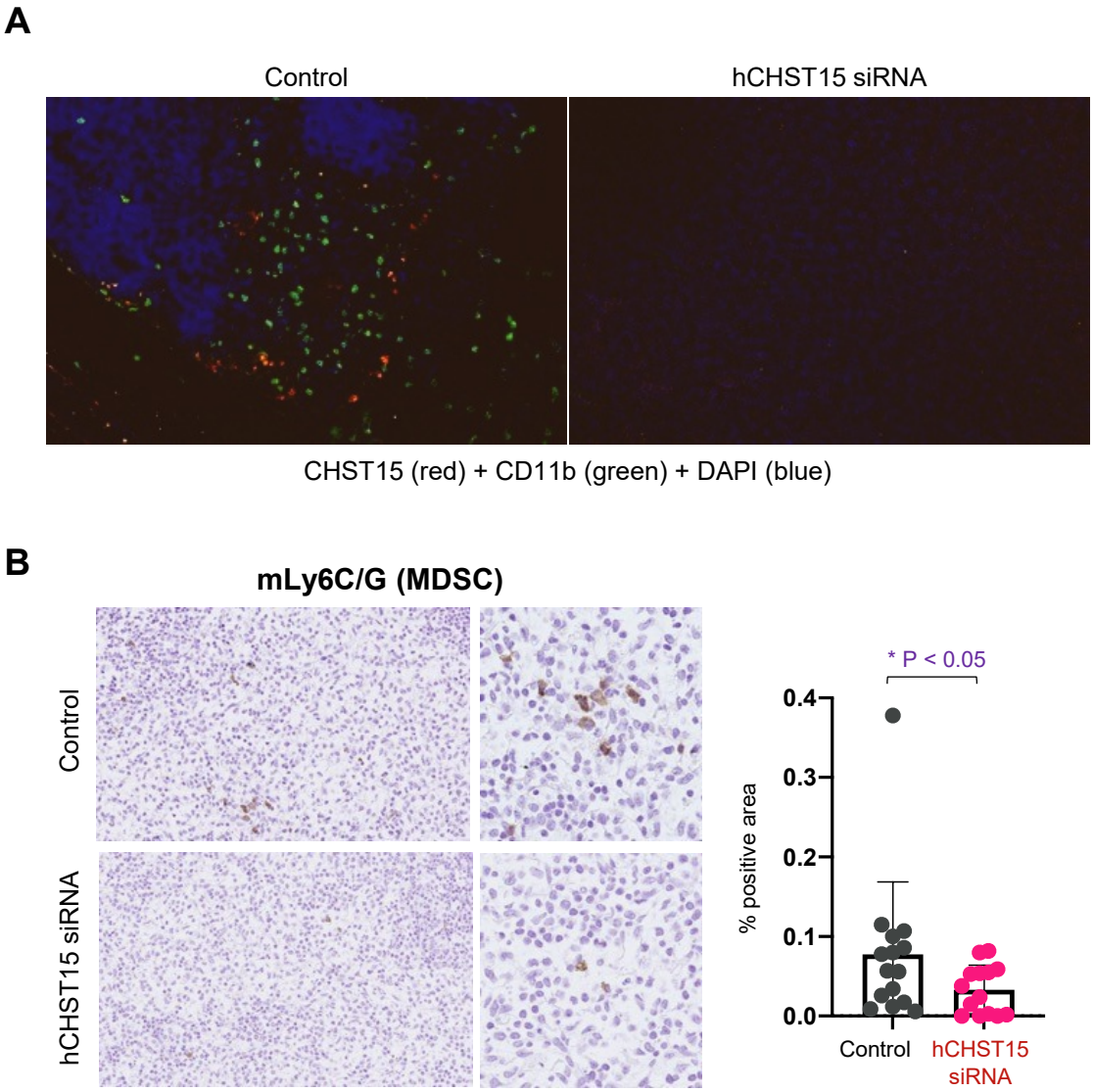

Figure S4. Part of TLDN MDSC expressed CHST15 and hCHST15 siRNA repressed MDSCs in the TDLN. **A.** Immunostaining for CHST15 (red) and CD11b (green) with DAPI (blue) in the TDLN of KPC mice treated with control (left panel) or hCHST15 siRNA (right panel). Original magnification, x200. **B:** Immunostaining for Ly6C/G (brown) in the TDLN of BxPC-3 mice treated with control (upper panel) or hCHST15 siRNA (lower panel). Original magnification, x200 (left), x630 (right). Quantitative analysis for stained tissues of control- (black dot) or hCHST15 siRNA (red bot)-treated mice. Percentage positive areas for Ly6C/G are shown. Mean ± SD (n=15). *p < 0.05 by independent t test.

References

1. Ye, J., Suizu, F., Yamakawa, K., Mukai, Y., Kato, M., Yoneyama, H., Yahagi, N., and Matsuda, Y. (2023). Silencing of tumoral carbohydrate sulfotransferase 15 reactivates lymph node pancreatic cancer T cells in mice. Eur J Immunol *53*, e2250160. 10.1002/eji.202250160.
2. Suzuki, K., Arumugam, S., Yokoyama, J., Kawauchi, Y., Honda, Y., Sato, H., Aoyagi, Y., Terai, S., Okazaki, K., Suzuki, Y., et al. (2016). Pivotal Role of Carbohydrate Sulfotransferase 15 in Fibrosis and Mucosal Healing in Mouse Colitis. PLoS One *11*, e0158967. 10.1371/journal.pone.0158967.
3. Takakura, K., Shibazaki, Y., Yoneyama, H., Fujii, M., Hashiguchi, T., Ito, Z., Kajihara, M., Misawa, T., Homma, S., Ohkusa, T., et al. (2015). Inhibition of Cell Proliferation and Growth of Pancreatic Cancer by Silencing of Carbohydrate Sulfotransferase 15 In Vitro and in a Xenograft Model. PLoS One *10*, e0142981. 10.1371/journal.pone.0142981.
4. Chen, C., Ridzon, D.A., Broomer, A.J., Zhou, Z., Lee, D.H., Nguyen, J.T., Barbisin, M., Xu, N.L., Mahuvakar, V.R., Andersen, M.R., et al. (2005). Real-time quantification of microRNAs by stem-loop RT-PCR. Nucleic Acids Res *33*, e179. 10.1093/nar/gni178.
5. Foster, D.J., Brown, C.R., Shaikh, S., Trapp, C., Schlegel, M.K., Qian, K., Sehgal, A., Rajeev, K.G., Jadhav, V., Manoharan, M., et al. (2018). Advanced siRNA Designs Further Improve In Vivo Performance of GalNAc-siRNA Conjugates. Mol Ther *26*, 708-717. 10.1016/j.ymthe.2017.12.021.

6. Guo, X., Zhao, Y., Nguyen, H., Liu, T., Wang, Z., and Lou, H. (2018). Quantitative Analysis of Alternative Pre-mRNA Splicing in Mouse Brain Sections Using RNA In Situ Hybridization Assay. J Vis Exp. 10.3791/57889.

7. Wu, S., Shi, X., Si, X., Liu, Y., Lu, T., Zhang, L., Liang, Z., and Zeng, X. (2019). EGFR T790M detection in formalin-fixed paraffin-embedded tissues of patients with lung cancer using RNA-based in situ hybridization: A preliminary feasibility study. Thorac Cancer *10*, 1936-1944. 10.1111/1759-7714.13169.